Applied Energy 341 (2023) 121072

Contents lists available at ScienceDirect

Applied Energy

journal homepage: www.elsevier.com/locate/apenergy

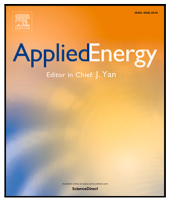

Modeling of a hinged-raft wave energy converter via deep operator learning and wave tank experiments

Jincheng Zhang [a], Xiaowei Zhao [a,*], Deborah Greaves [b], Siya Jin [b]

[a] Intelligent Control & Smart Energy (ICSE) Research Group, School of Engineering, University of Warwick, Coventry, UK
[b] School of Engineering, Computing and Mathematics, University of Plymouth, Plymouth, UK

ARTICLE INFO

Keywords:
Data-based modeling
Deep learning
DeepONet
Wave energy converter
Wave tank experiment

ABSTRACT

Model identification for a hinged-raft wave energy converter (WEC) is investigated in this paper, based on wave tank experiments and deep operator learning. Different from previous works which all formulated this issue as a function approximation task, this work, for the first time, formulates it as an operator approximation task (which learns the mapping from a function space to another function space). As such, a continuous-time WEC model is identified from data, greatly expanding the horizon of data-based WEC modeling because previous works were limited to discrete-time model identification. The error accumulation for multi-step predictions in the discrete-time formulation is thus also addressed. The model is developed by first carrying out a set of wave tank experiments to generate the training data, and then the deep operator learning model, i.e. the DeepONet, is constructed and trained based on the experimental data. The validation study shows that the model captures the WEC dynamics accurately. A new set of experimental runs are further carried out and the results show that after training, the model can be used as a digital wave tank, an alternative to the expensive numerical and physical wave tanks, for accurate and real-time simulations of the WEC dynamics.

1. Introduction

Wave energy, along with other offshore renewable energies (ORE) such as offshore wind and tidal, plays an important role in the global transition to net zero. To enable efficient extraction of power from waves, different types of wave energy converters (WEC), such as oscillating water columns [1], point absorbers [2,3], and hinged raft devices [4], have been developed. Various test studies have been carried out to evaluate the WECs' performance, based on numerical wave tank (NWT) [5], physical wave tank (PWT) [6], and real-sea site tests [7]. However, due to the complexity of the underlying hydrodynamics, it is still a difficult and complicated task to accurately model the dynamic motions of the WEC devices, which, on the other hand, is very important for the further reduction of the cost of wave power, in the scenarios such as power take-off evaluation [8], fatigue assessment [9], and WEC control [10,11].

The CFD models [12], which solve the Navier–Stokes (NS) equations using numerical methods, are developed to accurately model the dynamical behaviors of the WECs. These models, which are accurate in capturing complex nonlinear hydrodynamics, are, however, computationally expensive. For example, a typical simulation for a simulation time of 1 h would require a computational time of 1000 h [13]. To alleviate the computational burden, models based on potential flow theory (PFT) are developed [14]. Although they are more efficient than CFD models, various assumptions are made which undermines their accuracy and limits their use in strongly nonlinear scenarios [15]. Moreover, for a specific WEC device under investigation, extensive modeling and calibration efforts are needed in order to balance the computational costs and the model accuracy.

To alleviate the physics-based WEC modeling burden, the development of system identification (SID) methods based on numerical/experimental wave tank data is also gaining attention. In [13,16], modeling of a test WEC device, i.e. an infinitely long horizontal bar, was investigated based on NWT data, where several linear and nonlinear SID methods were employed including the linear autoregressive with exogenous input model (ARX), the Kolmogorov-Gabor polynomial model (KGP), and the multi-layer perceptron (MLP). In [17], a scaled Wavestar point absorber WEC was modeled based on the PWT experimental data, where the ARX model and the nonlinear KGP model were employed. The models developed in these works showed that the data-based modeling approaches achieved very promising performance in predicting the nonlinear dynamical behaviors of the WECs. However, as they were either based on traditional SID methods or simple machine

* Corresponding author.
E-mail addresses: jincheng.zhang.1@warwick.ac.uk (J. Zhang), xiaowei.zhao@warwick.ac.uk (X. Zhao), deborah.greaves@plymouth.ac.uk (D. Greaves), siya.jin@plymouth.ac.uk (S. Jin).

https://doi.org/10.1016/j.apenergy.2023.121072
Received 18 September 2022; Received in revised form 17 March 2023; Accepted 1 April 2023
Available online 14 April 2023

learning (ML) methods, their ability in handling very complex systems is limited. More importantly, in these works, the dynamic modeling of the WEC was all formulated as a function approximation task where the aim was to predict the state of the WEC at a future time instant based on the excitation signals and the historical states of the WEC. Under this kind of formulation, though the single-step prediction can be achieved accurately, the error accumulation is inevitable for multi-step predictions [17].

This paper focuses on the development of a novel dynamic model for a hinged-raft WEC based on wave tank experimental data, which can address the above-mentioned limitations of existing data-based WEC modeling methods. Particularly, a novel deep learning method is employed in this work following the deep operator learning framework [18]. By leveraging on the power of deep learning, the developed model is designed to handle systems of great complexity, while by formulating the issue of WEC modeling as operator learning instead of function approximation, the developed model is designed to take advantage of the underlying data structure and, at the same time, avoid the accumulative errors which are present in existing works. The development of operator learning has recently emerged. Yet a few exciting successes have been seen in various application areas, such as in the multi-scale bubble dynamics [19], the electroconvection multi-physics fields [20], the high-speed flows [21], and the inference of the solution of parametric partial differential equations [22]. In this paper, we adopt the operator learning strategy, i.e. the deep operator networks (DeepONet) [18], for the modeling of the dynamic motions of offshore structures for the first time. We mention that this work, which is based on operator learning (i.e. the learning of the mapping from a function space to another function space), is distinct from the previous ML-based works on offshore structures, such as the modeling of ship motions [23] and floating structures [24] using recurrent neural networks (RNN), which were all in the traditional paradigm of function approximation. Particularly, the traditional ML paradigm of function approximation requires the discretization and evaluation of the structural dynamics at all the discrete time instants. This, on the other hand, is not required by the operator learning approach. Moreover, after training, the DeepONet can make prediction with any continuous time coordinate t as the input, while the function approximation approaches can only make predictions at fixed discrete time instants. A more detailed comparison of DeepONet with function approximation ML models can be referred to [25,26].

The detailed model structure in this work follows the DeepONet framework, which consists of two networks, i.e. a branch net and a truck net. The branch net is employed to process the input function which is the wave elevation profile during a certain time period, while the truck net is employed to process the output function which is the continuous-time WEC response. In this way, the underlying data structure is embedded in the network structure, thus guaranteeing a good generalization performance. Furthermore, based on the original DeepONet structure, the network in this work is designed to treat the initial condition of the dynamical system and the input function by two sub-networks, so that different input features are processed by separate paths. The DeepONet model is then trained to approximate the dynamics of a hinged-raft WEC based on wave tank experimental data. First, a set of wave tank experiments are carried out for a range of sea conditions where the dynamic motion of the WEC and the wave elevations are measured. The Ocean Basin [27] at the University of Plymouth, which has been used previously for various studies in wave energy [28,29] and tidal energy [30], is used for carrying out the experiments. Then based on the experimental data, the operator learning model is trained to approximate the WEC dynamics. The output of the operator learning model is the function of the time coordinate to the WEC state (hereby denoted as $\mathbf{y}(t)$), while the input of the operator learning model is the function of the time coordinate to the wave elevations (hereby denoted as $u(t)$).

Table 1
The advantages of the dynamic model developed in this work based on DeepONet compared with existing works in the literature.

Method	Error accumulation	Problem formulation	Model type
ARX	Yes	Function approximation	Discrete-time
KGP	Yes	Function approximation	Discrete-time
MLP	Yes	Function approximation	Discrete-time
RNN	No	Function approximation	Discrete-time
DeepONet	No	Operator approximation	Continuous-time

After training, the performance of the data-based WEC model is first evaluated using the test dataset that is kept away from the training process. The results show that the model is able to achieve accurate prediction of the WEC motions in real time. A set of new experimental runs are then carried out to further demonstrate the model's accuracy and its generalization ability. The results show that for all the considered cases and all the DoFs of the WEC, the maximum prediction error is just 6.3% of the corresponding value range. This fully demonstrates the applied value of the developed data-based WEC model, as it shows that once the wave tank data is obtained and the training is complete, the model can be used to predict the dynamic motions of the WEC under new wave conditions, effectively serving as an accurate and efficient alternative to the PWT and the NWT which are both very expensive.

Furthermore, in addition to the DeepONet approach, a set of function approximation approaches, including the linear model (LM), the multi-layer perceptron (MLP), the convolutional neural networks (CNN), the long short-term memory (LSTM) and the gated recurrent unit (GRU), are also implemented in this work for comparison, even though the data requirement for these traditional approaches is much more strict than the DeepONet approach. Specifically, the training data for these approaches is the full measurements of the WEC motions at all the discretized time instants, while the training data for the DeepONet is the partial measurements of the WEC motions at randomly sampled time instants. The results show that compared with these traditional approaches, the DeepONet not only predicts the WEC motions more accurately with less training data requirement, but also achieves the prediction of the WEC motions at any continuous time instants while the other approaches can only predict the WEC motions at pre-defined discrete time instants.

The main contributions and novelties of this work are summarized as follows:

(1) **A novel dynamic model of a hinged-raft wave energy converter is developed based on deep operator learning and wave tank experiments. To the best of the authors' knowledge, this is for the first time that a continuous-time WEC model is identified from data.** The developed model addresses the limitation of previous data-based WEC models, by taking advantage of the power of deep learning in tackling a system of high complexity and the power of operator learning in making use of the underlying data structure to achieve accurate long-term predictions. The comparison of this work with existing works in the literature is summarized in Table 1.

(2) **Different from previous machine learning based works in the modeling of wave energy devices and other offshore structures, which are all formulated as function approximation task, this work, for the first time, explores the use of the operator learning approach (which learns the mapping from a function space to another function space) for ocean structure modeling.** The proposed approach follows the recently-proposed DeepONet framework and an efficient way to process the WEC's initial condition is also designed in the network structure.

(3) **A set of wave tank experiments are carried out to generate the dataset of wave elevations and the corresponding dynamic motions of the prototype hinged-raft WEC.** This

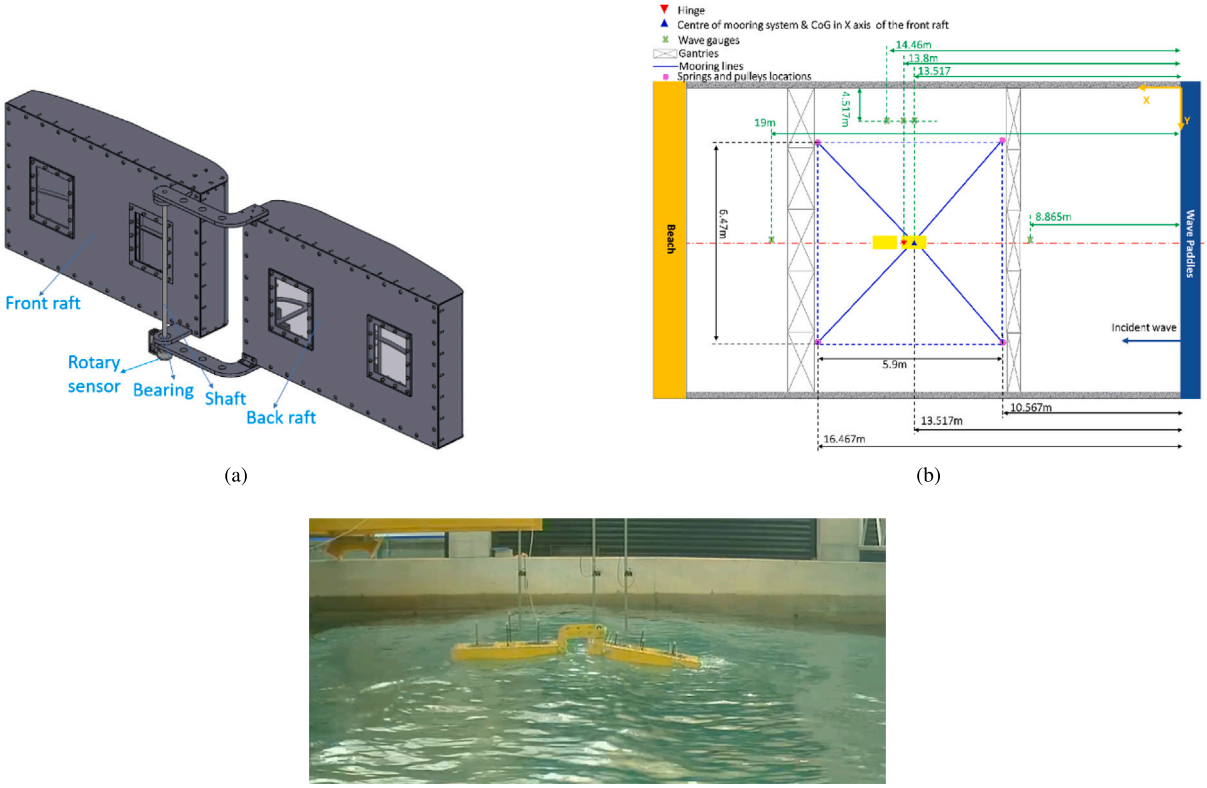

Fig. 1. The setup of the wave tank experiments: (a) the illustration of the scaled (1:50) hinged-raft WEC investigated in this work; (b) the illustration of the model test set up in the Ocean Basin; (c) a snapshot of the hinged-raft WEC at a typical time instant during an experimental run.

extensive set of experiments provides a realistic approximation of the WEC operation at real-sea conditions, vital for the deployment of the developed WEC model in the future.

(4) **The developed model's performance is first evaluated by comparing the prediction results with the data that are kept away from the training process. Then the evaluation under new experimental runs is carried out. The results show that the developed model is able to predict the dynamic responses of the WEC very accurately in real time, for both the test dataset and the new experimental runs.** Therefore, after training, it can effectively serve as a digital wave tank (DWT), i.e. an accurate and efficient alternative to the expensive numerical and physical wave tanks.

The remaining part of this paper is organized as follows: the dynamic modeling of the hinged-raft WEC based on wave tank experimental data is described in Section 2. The developed WEC model's performance is then extensively evaluated in Section 3. Finally the conclusions are drawn in Section 4.

2. Methodology

The data-driven dynamic modeling of a WEC aims at developing a model that can predict the structural response of the WEC given an excitation signal (e.g. the wave elevation profile) as the input. This problem may be formulated as function approximation task, by discretizing the time coordinate and then employing a traditional ML model, such as a seq-to-seq model [31], to predict the WEC responses at a sequence of discrete time instants based on the sequence of excitation signals. This, however, has several limitations such as the strict requirement of data gathering. In this work, to take advantage of the underlying data structure, we tackle the WEC modeling issue by formulating it as an operator approximation task. More detailed comparison between function approximation and operator approximation ML approaches can be found in Table 2 of Ref. [25] and in Table 3 of Ref. [26].

Specifically, denote the external excitation signal as $u(t)$ and the variable characterizing the WEC's structural motions as $\mathbf{y}(t)$. The WEC modeling problem can then be formulated as how to approximate the operator $\mathscr{G}$, which takes the function $u(t)$ as the input and returns the function $\mathbf{y}(t)$ as the output, i.e.

$$\mathbf{y}(t) = \mathscr{G}(u)(t), \tag{1}$$

based on a set of training data gathered via wave tank experiments. In the following parts, the wave tank experiments are described first. Then the operator approximation network, hereby denoted as $\hat{\mathscr{G}}$, are presented in detail.

2.1. Wave tank experiments

The wave tank experiments are carried out at the Ocean Basin [27] at the University of Plymouth, which has been used in various experimental studies for wave energy research, other ORE and coastal and ocean engineering applications. The wave tank's length is 35 m and its width is 15.5 m. It has an adjustable floor that allows different operating water depths up to 3 m. For all the experimental runs in this work, the operating water depth is set as 1.5 m. The WEC device under investigation is a scaled (1:50) hinged-raft WEC, which is illustrated in Fig. 1(a). It consists of a front raft and a back raft which are connected together via the shaft. A top view of the model test set up in the wave tank is illustrated in Fig. 1(b), where the WEC location, the mooring lines, and the wave gauge locations are shown. A snapshot of the hinged-raft WEC in the wave tank at a typical time instant during one experimental run is shown in Fig. 1(c). As shown, under uni-directional wave excitation, the main dynamics of the hinged-raft WEC are the whole structure's vertical movement, the front raft' pitch motion, and

Table 2
The sea conditions investigated in this work.

Sea condition	Scale model (1/50)		Full model	
	Hs [m]	Tp [s]	Hs [m]	Tp [s]
#1	0.05	1.1	2.5	7.78
#2	0.22	2.2	11	15.56

the back raft's pitch motion. The WEC motions are therefore mainly characterized by these three DoFs.

A set of experimental runs are carried out in this work in order to cover a range of wave scenarios corresponding to typical sea conditions. The environmental characterization is derived based on the data provided by ECMWF [32]. Specifically, two sea conditions are considered, and for each sea condition, 10 experimental runs are carried out with two different peak enhancement factors (i.e. $\gamma = 1$ and $\gamma = 3.3$) and five different random wave phases. Thus a total number of 20 experimental runs are carried out. The wave parameters of the corresponding sea conditions are reported in Table 2, where the sea condition #1 and #2 represent, respectively, the typical and extreme conditions during a 50-year return period for the EMEC site off Scotland. The JONSWAP spectrum is used as the wave spectrum. The interested reader may refer to [33] for further details regarding the environmental characterization. Furthermore, each experimental run is carried out for about 9.5 min which corresponds to about 1.1 h at full scale. During the experiments, wave gauges are used to measure the wave height at a frequency of 128 Hz, while the structure motions (including all the six DoFs of each raft) are captured by the infrared marker-based motion capture system at a frequency of 128 Hz. The wave data at the WEC locations, which is the training input, and the structural motion data, which is the training output, are collected and used to train the operator approximation network $\hat{\mathscr{G}}$.

2.2. DeepONet structure and training

To approximate the operator $\mathscr{G}$ based on the data gathered from the wave tank experiments, an operator approximation ML model is constructed in this section following the DeepONet proposed in [18]. The DeepONet is based on rigorous mathematical theory of universal approximation of nonlinear continuous operators proposed in [34], where the authors in [18] extended it to deep neural networks. The DeepONet consists of a branch net and a trunk net. The branch net takes the input function, i.e. the function $u(t)$ in this work, as the input, and returns an output vector $\mathbf{b}$. The trunk net takes the input of the output function, i.e. the continuous time coordinate t in this work, as the input, and returns an output vector $\mathbf{a}$. The output of the output function, i.e. the WEC state at the time t in this work, is finally obtained by the dot product of the vectors $\mathbf{b}$ and $\mathbf{a}$. In this work, the network structure of the DeepONet is further modified to take account of the initial condition of the hinged-raft WEC. The overall network structure is illustrated in Fig. 2. As shown, the trunk net is the same as in the original DeepONet, while the branch net consists of two sub-networks which are designed to process the input function and the initial condition of the WEC via separate paths, as they contain different features. Denote the input–output mapping of the Trunk Net as $\mathscr{T}$. Denote the input–output mapping of the Branch Net 1 and the Branch Net 2 as $\mathscr{B}_1$ and $\mathscr{B}_2$ respectively. The DeepONet model can then be expressed as

$$\begin{aligned}
&\mathbf{b}_1 = \mathscr{B}_1(\hat{\mathbf{u}}),\\
&\mathbf{b} = \mathscr{B}_2([\mathbf{b}_1, \mathbf{y}_0]),\\
&\mathbf{a} = \mathscr{T}(t)\\
&\hat{\mathscr{G}}_{\mathbf{y}_0}(u)(t) = \langle \mathbf{a}, \mathbf{b} \rangle + b_0
\end{aligned} \tag{2}$$

where $\hat{\mathbf{u}}$ is the discrete representation of the input function $u(t)$, $\mathbf{y}_0$ is the initial condition of the WEC, and $\langle , \rangle$ represents the dot product. The training variable of the DeepONet thus consists of the training variables in all the sub-networks including $\mathscr{T}$, $\mathscr{B}_1$, $\mathscr{B}_2$ and the bias term b_0. All the sub-networks in this work are further specified as fully-connected neural networks, as is in [18].

Algorithm 1 The training and prediction procedure

```
% The DeepONet training
Load the wave elevation data.
Load the corresponding WEC structural motion data.
Preprocess the wave and the WEC data via standard scalers.
Set the batch size N_b.
Set the early-stopping patience number N_p.
while True do
    Extract a random batch of training data pairs {[y_0^i, û^i, t^i; y(t^i)], 1 ≤ i ≤ N_b}.
    Train the DeepONet by feeding the data batch to minimize the training loss 𝒮.
    if the early-stopping patience number is reached then:
        Break
    end if
end while
% The DeepONet prediction
Specify a wave elevation profile of interest û*.
Specify the initial condition of the WEC y_0*.
Specify a set of time coordinates of interest [t_1, t_2, .., t_M].
for i in [1,2,...,M] do
    Propagate [y_0*, û*, t_i] through DeepONet to predict y(t_i).
end for
The dynamic motions of the WEC at all the time coordinates [t_1, t_2, .., t_M] are obtained.
```

The training of the DeepONet model is then carried out in supervised manner, i.e., given an input data tuple $[\hat{\mathbf{u}}^i, \mathbf{y}_0^i, t^i]$, the DeepONet is trained to approximate the training target $\mathbf{y}(t^i)$. The training loss function is specified as the mean squared error between the DeepONet output and the training target, which is expressed as

$$\mathscr{L} = \frac{1}{N_b}\sum_{i=1}^{N_b}(\hat{\mathscr{G}}_{\mathbf{y}_0^i}(\hat{\mathbf{u}}^i)(t^i) - \mathbf{y}(t^i))^2. \tag{3}$$

Here $\{[\mathbf{y}_0^i, \hat{\mathbf{u}}^i, t^i; \mathbf{y}(t^i)], 1 \le i \le N_b\}$ represents a batch of training data pairs where N_b is the batch size. The Adam optimizer [35] is then used for the training, by feeding the data batch to the DeepONet to minimize the loss function $\mathscr{L}$. After training, the WEC state at a given time instant t^* under a new wave excitation can be predicted by propagating the new wave elevation profile $\hat{\mathbf{u}}^*$, the WEC initial state $\mathbf{y}_0^*$, and the time coordinate t^* through the DeepONet. Similarly, the dynamic WEC motions during a period of time can be obtained by considering a set of time coordinates. The detailed training and prediction procedure is summarized below as Algorithm 1. It is worth mentioning that the input of the Trunk Net is the continuous-time coordinate t. Thus the WEC model identified in this work is a continuous-time model. Therefore, this work greatly expands the horizon of data-based WEC modeling, as the previous works were all limited to the identification of discrete-time WEC models.

2.3. WEC modeling via function approximation approaches

In order to demonstrate the performance of the developed DeepONet-based WEC model, a set of function approximation approaches are also implemented in this work, where the input wave elevations and the output WEC dynamics are discretized at the same frequency and then the problem is formulated as how to approximate the function which takes the input wave elevation sequence and the initial WEC position as the input and returns the discretized WEC

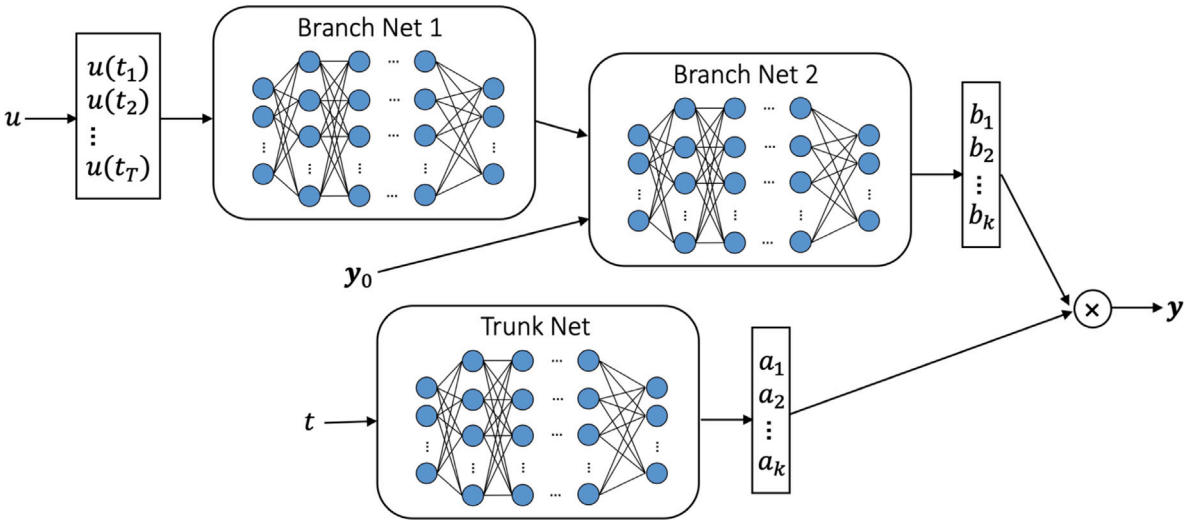

Fig. 2. The illustration of the DeepONet network structure.

motions as the output. A set of models, including the LM, the MLP, the CNN, the LSTM and the GRU, are employed for the function approximation task. In particular, for the LM and the MLP, the input is designed as the direct concatenation of the discrete wave elevations and the initial condition of the WEC, and the prediction target is set as the structural motions of the WEC at the same discrete time instants. As for the CNN, the LSTM, and the GRU, the initial condition of the WEC is treated as an additional feature and is concatenated with the wave elevation at each discrete time instant. In this way, the input is represented as a time series with multiple features. The CNN, LSTM, or GRU layer is then used to process the concatenated features at each time instant, and the processed features are fed into a fully-connected layer for the model output. The training of these function approximation models is finally carried out using the full measurement data of the WEC motions at all the discrete time instants. After training, given a discrete-time wave elevation sequence as the test input, the WEC motions at the same discrete time instants can be predicted.

3. Results

This section is devoted to the evaluation of the developed data-based WEC model. In the following parts, the training details of the DeepONet are given first. Then the model's performance is extensively evaluated, based on the test dataset (which is kept away from the training process) and a new set of wave tank experimental runs.

3.1. Model training

In this work, the dynamic response of the WEC under uni-directional wave excitation is of primary interest. Under such excitation, the main DoFs of the WEC are the structure's vertical displacement z, the front raft's pitch angle θ^f, and the back raft's pitch angle θ^b. Therefore, the output function of the DeepONet is specified as $\mathbf{y}(t) = [z, \theta^f, \theta^b](t)$. Similarly the initial condition of the WEC is specified as $\mathbf{y}_0 = [z_0, \theta_0^f, \theta_0^b]$. The time domain of the WEC modeling is specified as 50 s in this work, which, on the one hand, is sufficient to capture the WEC dynamics under typical wave excitation, and on the other hand, is useful to show that the developed WEC model can be combined with a wave forecasting method to achieve the forecasting of the WEC motions. For example, the work in [36,37] shows that the 50-second ahead wave forecasting can be achieved with fairly good accuracy. Furthermore, the input function of the DeepONet is usually represented at the so-called sensor points [18]. In this work, the sensor points are specified as the uniform grid points with a grid size of 0.5 s.

The data gathered through the wave tank experiments, including the wave data and the structure motion data, are first pre-processed into full scale. The data for each experimental run thus corresponds to about 1.1 hours' WEC operation time at full scale. The data for the initial and the last 3 min are then discarded, avoiding the potential disturbances at the beginning and towards the end of the experiments. Therefore, for each experimental run, the dataset corresponding to a period of 1 h is collected. Then the dataset is divided into three parts, the training dataset (the first 60% time instants), the validation dataset (the 60%–80% time instants), and the test dataset (the last 20% time instants). The training dataset is used to train the DeepONet, while the validation dataset is used to determine the model hyperparameters (such as the number of layers and the neuron number of hidden layers) and to monitor the model overfitting during the training of the model. The final network structures used in this work are determined as 100–200-200, 203–200–200, and 1–200-200–600 for the Branch Net 1, the Branch Net 2, and the Trunk Net respectively. We mention that the output of the Trunk Net is reshaped to 200 × 3 before the dot product so that the shape of **a** and **b** match with each other. The training of the DeepONet is then carried out via the mini-batch gradient descent. The batch size is tuned as 4×10^4 and the learning rate of the Adam optimizer is set as 10^{-4}. An early-stopping procedure based on the validation loss is implemented to avoid overfitting and the early-stopping patience is set as 100 epochs.

The model is implemented using the deep learning library Keras [38] with Tensorflow backend [39]. The whole training process is completed after around 10^5 iterations, which takes about 5 h using one NVIDIA RTX 6000 GPU card. The training and validation losses during the training process are given in Fig. 3. As shown, the training process converges after around 8×10^4 iterations and further training does not improve the validation loss any further and leads to overfitting. Therefore, the training weight obtained after 8×10^4 iterations is restored and used for the final model prediction. After training, the predictions are carried out on a standard laptop i.e. a MacBook Pro with 2 GHz Quad-Core Intel CPU in this work. In particular, it requires about 0.04 s computational time to predict the WEC dynamics for a simulation time of 50 s, which demonstrates that the prediction of the WEC dynamics can be achieved in real-time by the developed model.

3.2. Model evaluation — test dataset

The DeepONet model is first evaluated using the test dataset, i.e. the last 720 s data for each experimental run. These data are assumed unknown during the training process. The predictions are carried out

Table 3
The prediction RMSEs of the developed WEC model, evaluated with the test dataset. The values normalized by the range of the corresponding quantities are also included.

Case	Hs	Tp	γ	Quantity	RMSE (% of range)					
					LM	MLP	CNN	LSTM	GRU	DeepONet
1	2.5 m	7.78 s	1	z (m)	0.401 (5.7%)	0.353 (5.0%)	0.331 (4.7%)	0.381 (5.4%)	0.388 (5.5%)	0.313 (4.4%)
				θ^f (°)	1.71 (5.7%)	1.48 (4.9%)	1.45 (4.8%)	1.67 (5.6%)	1.71 (5.7%)	1.31 (4.4%)
				θ^b (°)	0.731 (5.6%)	0.620 (4.7%)	0.578 (4.4%)	0.657 (5.0%)	0.670 (5.1%)	0.550 (4.2%)
2	2.5 m	7.78 s	3.3	z (m)	0.549 (6.9%)	0.445 (5.6%)	0.444 (5.6%)	0.452 (5.7%)	0.463 (5.8%)	0.393 (4.9%)
				θ^f (°)	2.33 (6.6%)	1.85 (5.3%)	1.97 (5.6%)	1.88 (5.3%)	1.94 (5.5%)	1.64 (4.6%)
				θ^b (°)	0.973 (6.8%)	0.779 (5.5%)	0.752 (5.3%)	0.791 (5.5%)	0.810 (5.7%)	0.687 (4.8%)
3	11 m	15.56 s	1	z (m)	1.02 (4.5%)	0.966 (4.2%)	0.946 (4.1%)	0.974 (4.2%)	0.962 (4.2%)	0.961 (4.2%)
				θ^f (°)	3.93 (7.1%)	3.59 (6.5%)	3.52 (6.4%)	3.63 (6.6%)	3.56 (6.4%)	3.48 (6.3%)
				θ^b (°)	1.76 (5.3%)	1.65 (5.0%)	1.60 (4.8%)	1.62 (4.9%)	1.59 (4.8%)	1.67 (5.0%)
4	11 m	15.56 s	3.3	z (m)	0.760 (3.2%)	0.728 (3.1%)	0.727 (3.1%)	0.754 (3.2%)	0.748 (3.2%)	0.732 (3.1%)
				θ^f (°)	2.78 (5.4%)	2.60 (5.0%)	2.62 (5.1%)	2.86 (5.5%)	2.84 (5.5%)	2.57 (5.0%)
				θ^b (°)	1.37 (4.2%)	1.28 (3.9%)	1.29 (4.0%)	1.28 (3.9%)	1.25 (3.8%)	1.30 (4.0%)

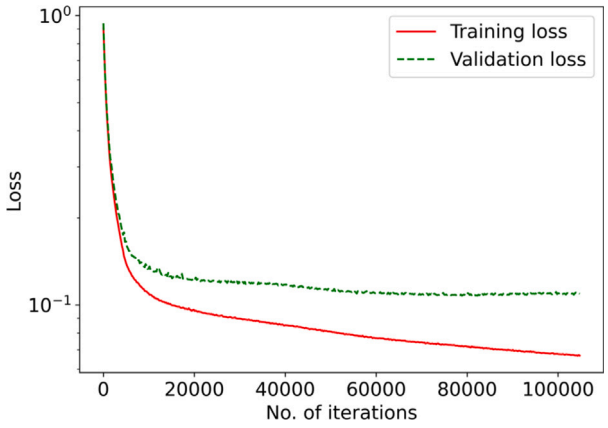

Fig. 3. The training and validation losses during the training process.

for all the 20 cases and then compared with the corresponding measurements obtained from the experiments. The results for four typical cases are given in Fig. 4 which correspond to different sea conditions (the sea conditions #1 and #2) and different peak enhancement factors ($\gamma = 1$ and $\gamma = 3.3$). The other 16 cases, where different random wave phases are used for wave generation, show similar prediction results as these four cases. Thus they are omitted here. As can be seen from Fig. 4, the WEC response predicted by the DeepONet matches very well with the experimental data throughout the time domain, for all the DoFs of the WEC including the vertical displacement, the front raft's pitch angle, and the back raft's pitch angle. This shows that the WEC dynamics are successfully captured by the DeepONet model. In particular, the prediction accuracy does not deteriorate with time, showing that the error accumulation, which was observed in previous works [17], is successfully tackled by the operator learning approach in this work. In addition, for different cases, the DeepONet shows consistent good performance, demonstrating that it is able to learn the WEC dynamics under various wave conditions.

It is worth mentioning that the model in this work is trained using mixed data from all the experimental runs. In this way, a single DeepONet model is trained for various sea states. An alternative training strategy is to train different ML-based models for different sea states with the corresponding data, such as in the wave prediction work in [40]. This kind of strategy may ease the training of the ML model, but each resulting model learns from the data corresponding to a specific sea state, thus limiting its flexibility for model interpolation/extrapolation. In [17], the training strategies of using single dataset and mixed dataset were both explored. The authors concluded that it was unclear which strategy is better for the models they constructed. In the present work, for the use of deep learning which is more data-intensive, the mixed training strategy is more advantageous as the access to the data obtained from all the experiments is particularly helpful to tackle overfitting and to enable efficient data mining.

Next, to quantify the model accuracy, the root mean square error (RMSE) of the prediction, which is defined as

$$\mathrm{RMSE} = \sqrt{\frac{1}{T}\sum_{i=1}^{T}(\hat{\mathbf{y}}(t_i) - \mathbf{y}(t_i))^2}, \tag{4}$$

is calculated. Here $\hat{\mathbf{y}}(t_i)$ and $\mathbf{y}(t_i)$ represent the prediction and the corresponding experimental measurement at the time t_i. The prediction RMSEs are then averaged over the cases with different random wave phases. The averaged RMSEs are given in Table 3, where the values normalized by the range of the corresponding quantities are also included. As shown, the prediction errors by the DeepONet model are very small for all the cases and for all the DoFs of the WEC. The maximum value of the normalized prediction errors is just 6.3%. Also, similar as the observation in Fig. 4, consistent good prediction accuracy is observed for different sea conditions, demonstrating the model's applicability to various sea states. Therefore, future work may involve the training of the DeepONet model with data from more cases covering more sea states, ultimately leading to a versatile data-based model for all kinds of sea conditions.

In addition, the predictions by other function approximation approaches (which can only predict the WEC motions at discrete time instants) are also carried out and the results are shown in Fig. 4. The corresponding prediction RMSEs are included in Table 3 for comparison. As shown, the DeepONet approach outperforms all these approaches. In particular, among all the employed approaches, the LM model is outperformed by the other approaches (which are all nonlinear), demonstrating the importance of modeling the nonlinear mapping relation. On the other hand, although all these discrete-time models are trained with the full measurements at all the time instants while the DeepONet is trained only with the partial measurements at the randomly-sampled time instants, the DeepONet still achieves higher accuracy than all of them.

3.3. Model evaluation - a new set of experimental runs

To further evaluate the performance of the developed data-based WEC model, four new wave tank experimental runs are carried out, which correspond to the four wave conditions reported in Table 3 but with different random wave phases for wave generation.

The WEC motions predicted by the DeepONet model are shown in Figs. 5 and 6, which correspond to the cases 1 and 4 in Table 3. The results for the other two cases are similar. Thus they are omitted here. As shown, the dynamic responses of the WEC predicted by the DeepONet match with the experimental data very well for the whole

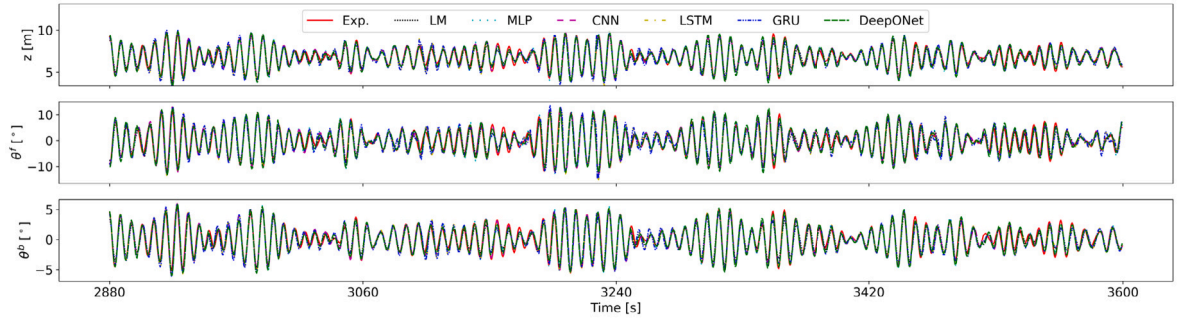

(a) Hs=2.5m, Tp=7.78s, γ=1

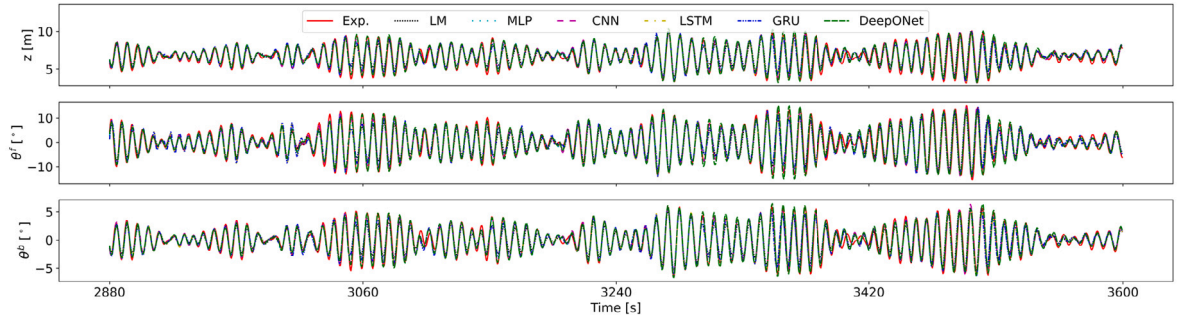

(b) Hs=2.5m, Tp=7.78s, γ=3.3

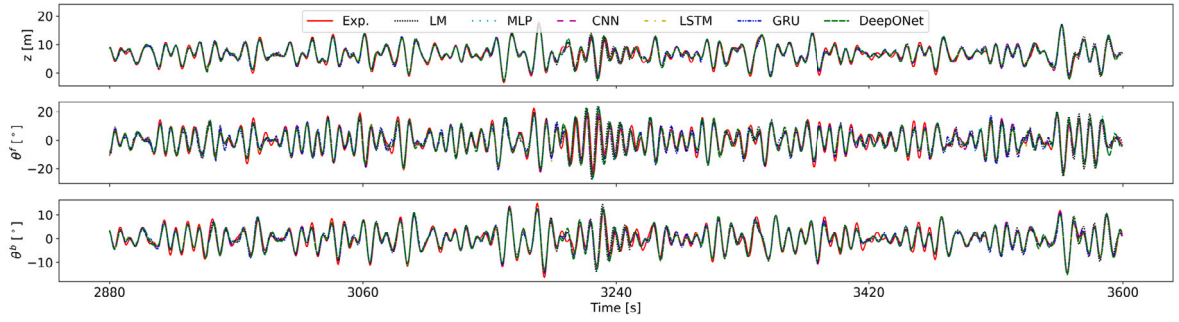

(c) Hs=11m, Tp=15.56s, γ=1

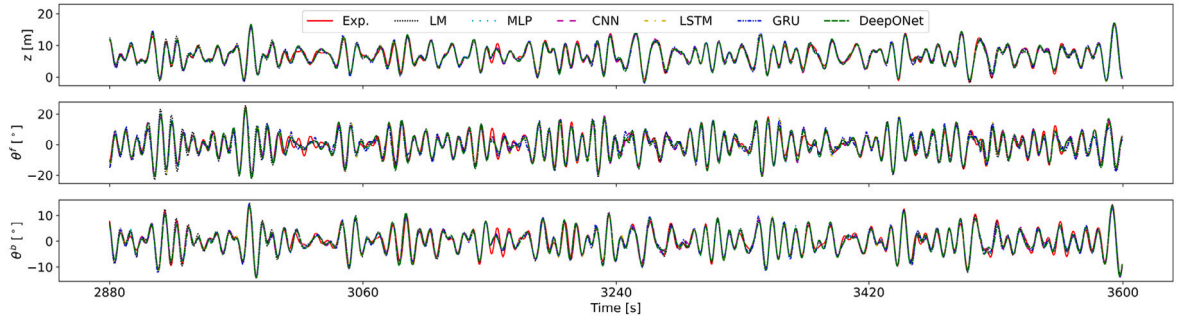

(d) Hs=11m, Tp=15.56s, γ=3.3

Fig. 4. The evaluation of the developed WEC model with the test dataset at four typical cases. The predictions by the developed WEC model, including the WEC's vertical displacement z, the front raft's pitch angle θ^f, and the back raft's pitch angle θ^b, are compared with the corresponding experimental data. The prediction results by other function approximation approaches are also shown.

time period of 3600 s. The prediction accuracy is then quantified by calculating the prediction RMSEs. The results are given in Table 4, where the results by all the other approaches are also included. As shown, the prediction errors by the DeepONet are very low for all the four cases and the DeepONet outperforms all the other approaches. The results here thus demonstrate that for a new case with a given wave elevation profile of interest, the dynamic motions of the WEC can be simulated accurately and efficiently by the developed model. Therefore, the developed model can be viewed as a digital wave tank (DWT), an alternative to the expensive numerical or physical wave tanks, for WEC simulations.

However, we mention that the developed model is based on data collected from either NWT or PWT. Therefore, it serves mainly as a way to fully explore the value of wave tank data, rather than replacing the NWT or PWT which is still essential for data generation. For example, for engineering applications, a large number of wave tank experiments

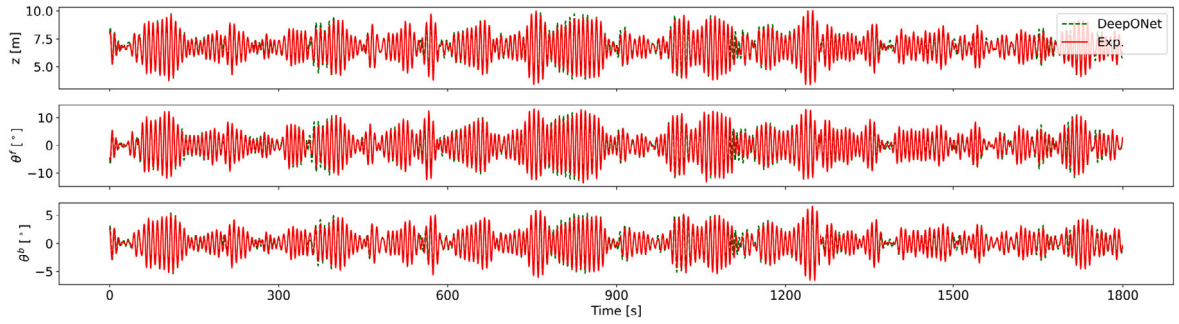

(a) Time: 0-1800s

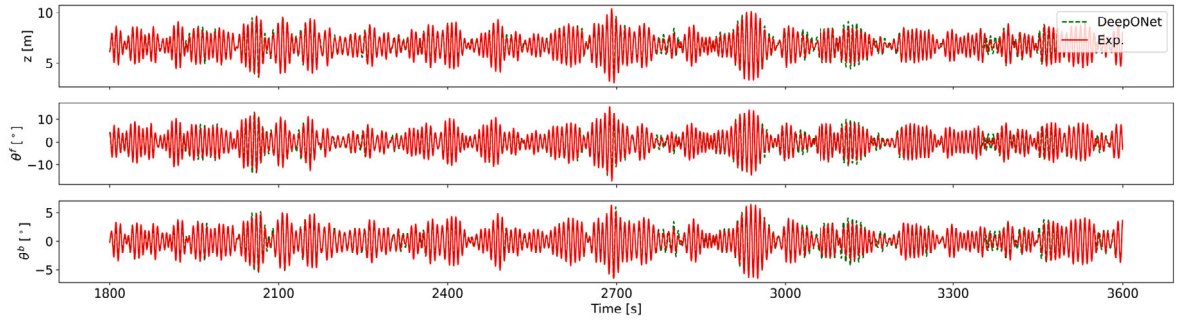

(b) Time: 1800-3600s

Fig. 5. The evaluation of the developed WEC model with the new set of experimental runs, at the wave parameters of Hs=2.5 m, Tp=7.78 s, γ=1.

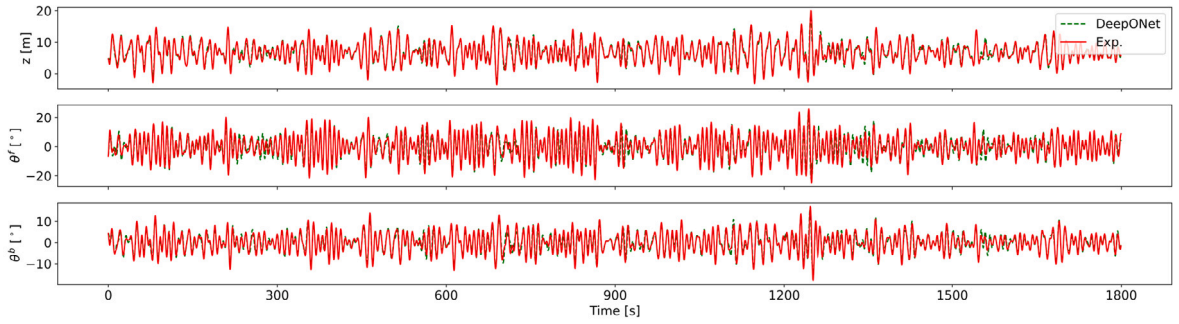

(a) Time: 0-1800s

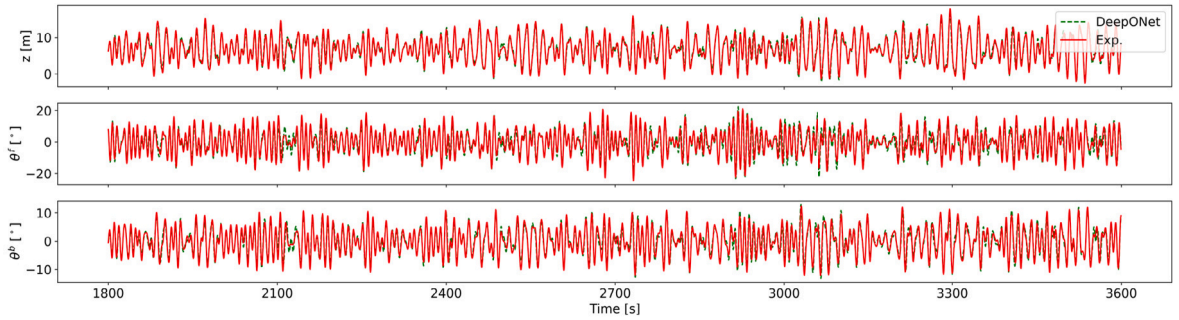

(b) Time: 1800-3600s

Fig. 6. The evaluation of the developed WEC model with the new set of experimental runs, at the wave parameters of Hs=11 m, Tp=15.56 s, γ=3.3.

are usually required to systematically investigate the WEC behaviors including its power-takeoff and structural fatigue. In such scenarios, a DeepONet model can be trained based on a reduced number of experiments and then employed to significantly augment the total number of the simulation cases, therefore reducing the cost of wave tank experiments.

Finally, to further illustrate the use of the developed model for WEC design and power prediction, the spectral response amplitude operator (RAO), which can be used to characterize the behavior of the WEC device, and the hinge position, which is directly related to the power generation of the hinged-raft WEC [4,41], are calculated and compared with the experimental results. The RAO is calculated as

Table 4
The prediction RMSEs of the developed WEC model, evaluated with the new set of experimental runs. The values normalized by the range of the corresponding quantities are also included.

Case	Hs	Tp	γ	Quantity	RMSE (% of range)					
					LM	MLP	CNN	LSTM	GRU	DeepONet
1	2.5 m	7.78 s	1	z (m)	0.387 (5.5%)	0.320 (4.5%)	0.299 (4.2%)	0.347 (4.9%)	0.348 (4.9%)	0.294 (4.2%)
				θ^f (°)	1.58 (5.3%)	1.31 (4.4%)	1.27 (4.2%)	1.53 (5.1%)	1.55 (5.2%)	1.24 (4.1%)
				θ^b (°)	0.704 (5.4%)	0.571 (4.4%)	0.520 (4.0%)	0.604 (4.6%)	0.608 (4.6%)	0.523 (4.0%)
2	2.5 m	7.78 s	3.3	z (m)	0.471 (5.9%)	0.369 (4.6%)	0.375 (4.7%)	0.379 (4.8%)	0.374 (4.7%)	0.360 (4.5%)
				θ^f (°)	1.89 (5.4%)	1.47 (4.2%)	1.55 (4.4%)	1.76 (5.0%)	1.71 (4.8%)	1.45 (4.1%)
				θ^b (°)	0.804 (5.6%)	0.624 (4.4%)	0.626 (4.4%)	0.658 (4.6%)	0.643 (4.5%)	0.606 (4.2%)
3	11 m	15.56 s	1	z (m)	1.02 (4.5%)	0.940 (4.1%)	0.925 (4.0%)	0.845 (3.7%)	0.858 (3.7%)	0.939 (4.1%)
				θ^f (°)	4.00 (7.2%)	3.59 (6.5%)	3.51 (6.3%)	3.24 (5.8%)	3.32 (6.0%)	3.52 (6.3%)
				θ^b (°)	1.77 (5.3%)	1.61 (4.8%)	1.59 (4.8%)	1.48 (4.5%)	1.47 (4.4%)	1.63 (4.9%)
4	11 m	15.56 s	3.3	z (m)	0.783 (3.3%)	0.702 (3.0%)	0.716 (3.0%)	0.706 (3.0%)	0.722 (3.0%)	0.696 (2.9%)
				θ^f (°)	2.78 (5.4%)	2.50 (4.8%)	2.51 (4.8%)	2.74 (5.3%)	2.77 (5.4%)	2.48 (4.8%)
				θ^b (°)	1.43 (4.4%)	1.26 (3.9%)	1.28 (3.9%)	1.24 (3.8%)	1.24 (3.8%)	1.27 (3.9%)

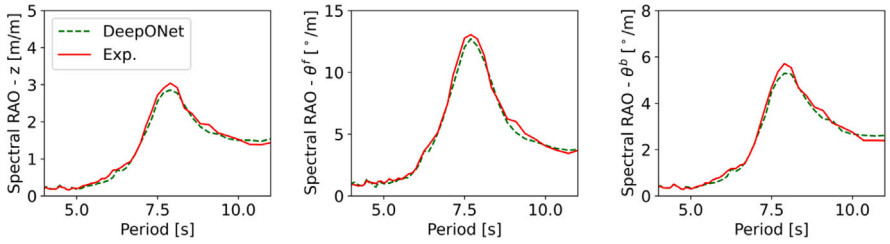

(a) Hs=2.5m, Tp=7.78s, γ=1

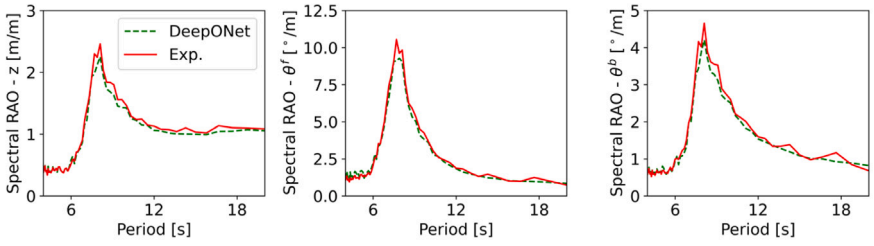

(b) Hs=11m, Tp=15.56s, γ=3.3

Fig. 7. The evaluation of the developed WEC model with the new set of experimental runs. The predictions by the developed WEC model, including RAO for the WEC's vertical displacement z, the front raft's pitch angle θ^f, and the back raft's pitch angle θ^b, are compared with the corresponding experimental results.

$$\text{RAO} = \sqrt{\frac{S_{DoF}}{S_u}} \tag{5}$$

where S_u and S_{DoF} represent the spectra of the wave and the corresponding DoF of the WEC. The results, including the spectral RAO predicted by the DeepONet and the experimental results, are given in Fig. 7 which correspond to the two cases shown in Figs. 5 and 6. The results for the other two cases are similar. Thus they are omitted here. As shown, the predictions match with the corresponding experimental results very well across the frequency range for all the DoFs including the vertical displacement of the WEC, the front raft's pitch motion, and the back raft's pitch motion. Next, the hinge position, which is defined as the angle between the front raft and the back raft, is calculated. The results are given in Figs. 8 and 9 which correspond to the two cases shown in Figs. 5 and 6. As shown, the responses of the hinge angle are predicted accurately by the DeepONet model, which demonstrates that the model can be used for power evaluation combining with a power take-off system.

4. Conclusion

The modeling of a hinged-raft WEC was investigated in this work, based on the wave tank experimental data and the deep operator learning approach. Different from the previous works which all formulated the data-based WEC modeling problem as function approximation task, this work, for the first time, formulated it as an operator approximation task. Under such formulation, the error accumulation issue for multi-step predictions in previous works was addressed, and a continuous-time WEC model was identified. Because previous works could only identify discrete-time models from data, this work expanded the horizon of data-based WEC modeling.

Specifically, a set of wave tank experiments for the hinged-raft WEC were first carried out to generate the wave and WEC motion data. Then the DeepONet, a recently-proposed operator learning framework based on rigorous mathematical theory, was employed and trained based on the experimental data. An efficient way to process the WEC's initial condition was also designed in the model structure. After training,

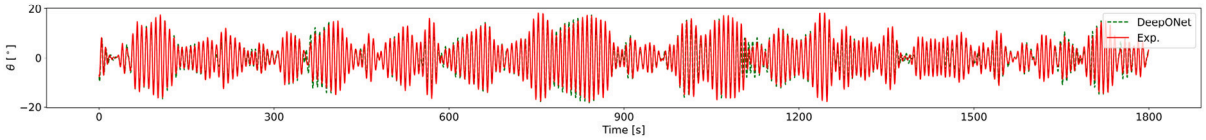

(a) Time: 0-1800s

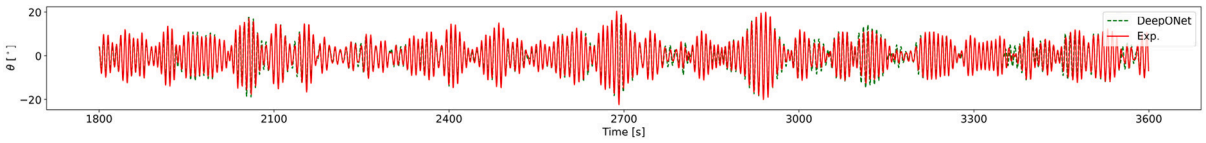

(b) Time: 1800-3600s

Fig. 8. The hinge position predicted by the developed WEC model at the new experimental run with the wave parameters of Hs=2.5 m, Tp=7.78 s, γ=1.

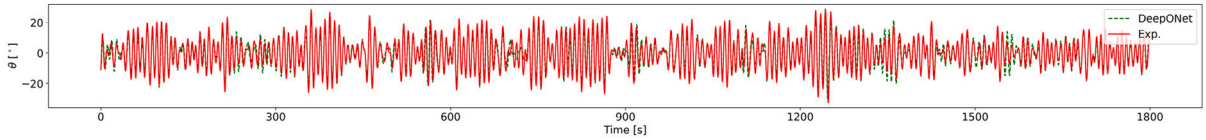

(a) Time: 0-1800s

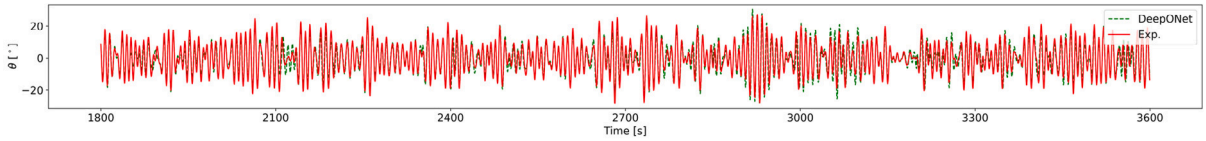

(b) Time: 1800-3600s

Fig. 9. The hinge position predicted by the developed WEC model at the new experimental run with the wave parameters of Hs=11 m, Tp=15.56 s, γ=3.3.

the model's performance was first evaluated by the test dataset. The results showed that it was able to achieve accurate prediction of the WEC dynamics in real time. Then a set of new experimental runs were carried out to demonstrate its use as an alternative to the expensive numerical or physical wave tanks for WEC simulations. The results showed that, after training, the model was able to achieve accurate and efficient predictions of the WEC dynamics with a given wave elevation signal as the input. In particular, among all the quantities and all the investigated cases, the maximum value of the prediction errors normalized by the value range was just 6.3%. Moreover, a comparison study with a set of function approximation approaches (including the linear model, the multi-layer perceptron, the convolutional neural networks, the long short-term memory, and the gated recurrent unit), was carried out. The results demonstrated the superiority of the DeepONet-based WEC model, in terms of its flexible data requirement, the prediction accuracy, and its ability of modeling the continuous-time instead of just the discrete-time WEC motions.

Future works may involve model training with more experimental data covering a wide range of sea states, ultimately leading to the establishment of a digital wave tank. It is also very interesting to investigate the application of the operator learning approaches to other types of WECs, and the integration of the identified model with other system components as well as its use for WEC control design. Another important aspect of data-based modeling is model interpretation. This is, however, extremely challenging for most deep learning models including both the traditional function approximation models and the DeepONet model in this work. With the current research efforts on model interpretation, an important future research direction is to make use of the data-based WEC model to derive new insights for WEC design and operation.

CRediT authorship contribution statement

Jincheng Zhang: Conceptualization, Data curation, Formal analysis, Investigation, Methodology, Project administration, Software, Validation, Visualization, Writing – original draft. **Xiaowei Zhao:** Conceptualization, Funding acquisition, Formal analysis, Investigation, Methodology, Project administration, Resources, Supervision, Writing – review & editing. **Deborah Greaves:** Funding acquisition, Investigation, Project administration, Resources, Supervision, Writing – review & editing. **Siya Jin:** Data curation, Investigation, Project administration, Writing – review & editing.

Declaration of competing interest

The authors declare that they have no known competing financial interests or personal relationships that could have appeared to influence the work reported in this paper.

Data availability

Data will be made available on request.

Acknowledgments

This work was supported by the UK Engineering and Physical Sciences Research Council (grant number: EP/S000747/1). The authors also acknowledge the Scientific Computing Research Technology Platform (SCRTP) at the University of Warwick for providing High-Performance Computing resources.

References

[1] Falcão AF, Henriques JC, Cândido JJ. Dynamics and optimization of the OWC spar buoy wave energy converter. Renew Energy 2012;48:369–81.

[2] Kramer M, Marquis L, Frigaard P. Performance evaluation of the wavestar prototype. In: 9th Ewtec 2011: Proceedings of the 9th European wave and tidal conference, southampton, UK, 5th–9th september 2011. University of Southampton; 2011.

[3] Guo B, Patton R, Jin S, Gilbert J, Parsons D. Nonlinear modeling and verification of a heaving point absorber for wave energy conversion. IEEE Trans Sustain Energy 2017;9(1):453–61.

[4] Davey T, Sarmiento J, Ohana J, Thiebaut F, Haquin S, Weber M, et al. Round robin testing: Exploring experimental uncertainties through a multifacility comparison of a hinged raft wave energy converter. J Mar Sci Eng 2021;9(9):946.

[5] Windt C, Davidson J, Ransley EJ, Greaves D, Jakobsen M, Kramer M, et al. Validation of a CFD-based numerical wave tank model for the power production assessment of the wavestar ocean wave energy converter. Renew Energy 2020;146:2499–516.

[6] Orphin J, Schmitt P, Nader J-R, Penesis I. Experimental investigation into laboratory effects of an OWC wave energy converter. Renew Energy 2022.

[7] Kofoed JP, Tetu A, Ferri F, Margheritini L, Sonalier N, Larsen T. Real sea testing of a small scale weptos WEC prototype. In: International conference on offshore mechanics and arctic engineering. vol. 51319, American Society of Mechanical Engineers; 2018, p. V010T09A022.

[8] Penalba M, Davidson J, Windt C, Ringwood JV. A high-fidelity wave-to-wire simulation platform for wave energy converters: Coupled numerical wave tank and power take-off models. Appl Energy 2018;226:655–69.

[9] Davidson J, Ringwood JV. Mathematical modelling of mooring systems for wave energy converters—A review. Energies 2017;10(5):666.

[10] Richter M, Magana ME, Sawodny O, Brekken TK. Nonlinear model predictive control of a point absorber wave energy converter. IEEE Trans Sustain Energy 2012;4(1):118–26.

[11] Li L, Gao Z, Yuan Z-M. On the sensitivity and uncertainty of wave energy conversion with an artificial neural-network-based controller. Ocean Eng 2019;183:282–93.

[12] Windt C, Davidson J, Ringwood JV. High-fidelity numerical modelling of ocean wave energy systems: A review of computational fluid dynamics-based numerical wave tanks. Renew Sustain Energy Rev 2018;93:610–30.

[13] Davidson J, Giorgi S, Ringwood JV. Identification of wave energy device models from numerical wave tank data—Part 1: Numerical wave tank identification tests. IEEE Trans Sustain Energy 2016;7(3):1012–9.

[14] Papillon L, Costello R, Ringwood JV. Boundary element and integral methods in potential flow theory: a review with a focus on wave energy applications. J Ocean Eng Mar Energy 2020;6(3):303–37.

[15] Penalba M, Giorgi G, Ringwood JV. Mathematical modelling of wave energy converters: A review of nonlinear approaches. Renew Sustain Energy Rev 2017;78:1188–207.

[16] Giorgi S, Davidson J, Ringwood JV. Identification of wave energy device models from numerical wave tank data—Part 2: Data-based model determination. IEEE Trans Sustain Energy 2016;7(3):1020–7.

[17] Giorgi S, Davidson J, Jakobsen M, Kramer M, Ringwood JV. Identification of dynamic models for a wave energy converter from experimental data. Ocean Eng 2019;183:426–36.

[18] Lu L, Jin P, Pang G, Zhang Z, Karniadakis GE. Learning nonlinear operators via DeepONet based on the universal approximation theorem of operators. Nat Mach Intell 2021;3(3):218–29.

[19] Lin C, Maxey M, Li Z, Karniadakis GE. A seamless multiscale operator neural network for inferring bubble dynamics. J Fluid Mech 2021;929.

[20] Cai S, Wang Z, Lu L, Zaki TA, Karniadakis GE. Deepm&mnet: Inferring the electroconvection multiphysics fields based on operator approximation by neural networks. J Comput Phys 2021;436:110296.

[21] Mao Z, Lu L, Marxen O, Zaki TA, Karniadakis GE. Deepm&mnet for hypersonics: Predicting the coupled flow and finite-rate chemistry behind a normal shock using neural-network approximation of operators. J Comput Phys 2021;447:110698.

[22] Wang S, Wang H, Perdikaris P. Learning the solution operator of parametric partial differential equations with physics-informed DeepONets. Sci Adv 2021;7(40):eabi8605.

[23] del Águila Ferrandis J, Triantafyllou MS, Chryssostomidis C, Karniadakis GE. Learning functionals via LSTM neural networks for predicting vessel dynamics in extreme sea states. Proc R Soc Lond Ser A Math Phys Eng Sci 2021;477(2245):20190897.

[24] Guo X, Zhang X, Tian X, Li X, Lu W. Predicting heave and surge motions of a semi-submersible with neural networks. Appl Ocean Res 2021;112:102708.

[25] Lu L, Meng X, Cai S, Mao Z, Goswami S, Zhang Z, Karniadakis GE. A comprehensive and fair comparison of two neural operators (with practical extensions) based on fair data. Comput Methods Appl Mech Engrg 2022;393:114778.

[26] Di Leoni PC, Lu L, Meneveau C, Karniadakis G, Zaki TA. Deeponet prediction of linear instability waves in high-speed boundary layers. 2021, arXiv preprint arXiv:2105.08697.

[27] Vyzikas T, Deshoulières S, Barton M, Giroux O, Greaves D, Simmonds D. Experimental investigation of different geometries of fixed oscillating water column devices. Renew Energy 2017;104:248–58.

[28] Portillo J, Collins K, Gomes R, Henriques J, Gato L, Howey B, et al. Wave energy converter physical model design and testing: The case of floating oscillating-water-columns. Appl Energy 2020;278:115638.

[29] Gomes RP, Gato LM, Henriques JC, Portillo JC, Howey BD, Collins KM, et al. Compact floating wave energy converters arrays: Mooring loads and survivability through scale physical modelling. Appl Energy 2020;280:115982.

[30] Brown S, Ransley E, Xie N, Monk K, De Angelis G, Nicholls-Lee R, et al. On the impact of motion-thrust coupling in floating tidal energy applications. Appl Energy 2021;282:116246.

[31] Sutskever I, Vinyals O, Le QV. Sequence to sequence learning with neural networks. Adv Neural Inf Process Syst 2014;27.

[32] ECMWF, ERA5. 2020, https://www.ecmwf.int/en/forecasts/datasets/reanalysis-datasets/era5.

[33] Tosdevin T, Jin S, Caio A, Simmonds D, Hann M, Greaves D. Extreme responses of a raft type WEC. In: The 14th European wave and tidal energy conference, Plymouth, UK. 2021.

[34] Chen T, Chen H. Universal approximation to nonlinear operators by neural networks with arbitrary activation functions and its application to dynamical systems. IEEE Trans Neural Netw 1995;6(4):911–7.

[35] Kingma DP, Ba J. Adam: A method for stochastic optimization. 2014, arXiv preprint arXiv:1412.6980.

[36] Duan W, Ma X, Huang L, Liu Y, Duan S. Phase-resolved wave prediction model for long-crest waves based on machine learning. Comput Methods Appl Mech Engrg 2020;372:113350.

[37] Zhang J, Zhao X, Jin S, Greaves D. Phase-resolved real-time ocean wave prediction with quantified uncertainty based on variational Bayesian machine learning. Appl Energy 2022;324:119711.

[38] Chollet F, et al. Keras. 2015, https://github.com/fchollet/keras.

[39] Abadi M, Agarwal A, Barham P, Brevdo E, Chen Z, Citro C, et al. TensorFlow: Large-scale machine learning on heterogeneous systems. 2015, Software available from tensorflow.org. https://www.tensorflow.org/.

[40] Law Y, Santo H, Lim K, Chan E. Deterministic wave prediction for unidirectional sea-states in real-time using artificial neural network. Ocean Eng 2020;195:106722.

[41] Zheng S, Zhang Y, Zhang Y, Sheng W. Numerical study on the dynamics of a two-raft wave energy conversion device. J Fluids Struct 2015;58:271–90.